

# THE INFLUENCE OF THE FIBRES ARRANGEMENT ON HEAT TRANSFER AND PRESSURE DROP OF POLYMERIC HOLLOW FIBRE HEAT EXCHANGERS

TEREZA KÚDELOVÁ\*, TEREZA KROULÍKOVÁ, ILYA ASTROUSKI,  
MIROSLAV RAUDENSKÝ

*Brno University of Technology, Faculty of Mechanical Engineering, Heat Transfer and Fluid Flow Laboratory, Technická 2896/2, Brno, Czech Republic*

\* corresponding author: [tereza.kudelova@vut.cz](mailto:tereza.kudelova@vut.cz)

**ABSTRACT.** Polymeric hollow fibre heat exchangers are the new alternative to common metal heat exchangers. These heat exchangers provide advantages, such as low weight, corrosion resistance, easy shaping and machining. Moreover, they consume less energy during their production. Therefore, they are environmentally friendly. The paper deals with shell & tube heat exchangers, which consist of hundreds of polymeric hollow fibres. The structure of the heat transfer surfaces has a significant influence on the effectivity of the use of the heat transfer area that is formed by the polymeric hollow fibres. The study gives a comparison of heat exchangers with an identical outer volume. The difference between them is in the structure of the heat transfer insert. One of the presented heat exchangers has fibres that are in-line and the second heat exchanger has staggered fibres. The study also pays attention to the difference in differential pressures caused by the difference in the structure of the heat transfer surfaces.

**KEYWORDS:** Polymeric hollow fibre, heat exchanger, heat transfer.

## 1. INTRODUCTION

Polymeric heat exchangers are an alternative to commonly used metal heat exchangers (HEs). The first attempts to construct a polymeric heat exchanger were made approximately 15 years ago [1]. Polymers bring advantages, such as low weight and low cost, and are also easily shaped and machined. A unit of mass of plastic requires half the energy than a unit of metal [1]. A low thermal conductivity - between  $0.1 \text{ Wm}^{-1}\text{K}^{-1}$  and  $0.4 \text{ Wm}^{-1}\text{K}^{-1}$  - is their main disadvantage [2].

Polymeric hollow fibre heat exchangers (PHFHEs) consist of hundreds or thousands of hollow fibres. The outer diameter of the fibres is around 1 mm and the thickness of the wall is approximately 10% of the outer diameter (it can vary if it is required by its application) [3]. Therefore, the disadvantage of the low thermal conductivity of the polymeric material is eliminated by the very thin fibre wall. Hollow fibres are potted together to create the heat transfer core. PHFHEs represent a very compact and effective heat exchanger. It is necessary to separate the fibres to guarantee the effective usage of the heat transfer area. The chaotization of the structure of PHFHEs and its influence on their intensification is studied in [4].

These heat exchangers are suitable for HVAC (heating, ventilating, and air conditioning) applications [5]. The condensation on the outer surface of PHFHE fibres and how the process is affected by the position of the heat exchanger is described in [6]. The authors describe the benefits of tilting the heat exchanger to the removal of the condensate. They also point out

the significance of the fibres's pitch. The PHFHE were tested in the standard conditions in air conditioning applications. The result shows that PHFHEs can be used in these applications.

The study of their suitability in the automotive industry is in [7]. The authors conclude that PHFHEs are able to achieve comparable results to the metal finned tube heat exchangers used nowadays. They also concluded that the low thermal conductivity is not an obstacle for their usage in the gas-liquid heat exchanger.

The possibility of their use as an immersed HE is presented in [8]. The studied PHFHEs showed overall heat transfer coefficients up to  $890 \text{ Wm}^{-2}\text{K}^{-1}$ . These results are competitive to commercially available immersed heat exchangers made of plastic.

Their fouling by the wastewater is described in [9]. The study compares fouling by shower wastewater and laundry wastewater. The fouling is strongly dependent on the type of wastewater. No significant decrease of overall heat transfer coefficient (OHTC) was observed when shower wastewater was used. Whereas, OHTC had only half of its original value after 35 days of exposure to laundry wastewater.

Their life expectancy is dealt with in [10]. The study proves that PHFHEs with a chaotic structure are able to withstand more than one million successful pressure cycles that simulate the operating conditions.

Another possible use of fibres is as a polymeric hollow fibre membrane. These are used for mass transfer e.g. filtration or distillation [11–13].

This study shows the influence of the fibre arrangement on the heat transfer and pressure drop of the PHFHE. The results show that it is possible to decrease the pressure drop by using suitable fibre arrangements.

## 2. EXPERIMENTAL SECTION

The paper deals with shell and tube PHFHEs, which differ in the fibre arrangement. Fibres are potted in a bundle that forms a heat transfer insert, which is placed in the stainless-steel shell.

Two HEs are compared, AB1 and AB2. Both are made of polycarbonate (PC) hollow fibres with an outer diameter of 0.8 mm. The thickness of the fibre wall was 10% of the outer diameter. HEs have a different structure of the heat transfer insert. AB1 has staggered fibres (the fibres form an angle of 45° across the layers). AB2 has all fibres in-line. This results in heat transfer inserts made of a different number of different lengths. However, the heat transfer area varies by 3.7% i.e. the HEs are comparable to each other and the influence of the fibre arrangement can be observed. Figure 1 shows the heat transfer surface and the completed HE. The properties of the tested samples are listed in Table 1.

All experiments were performed with cold water inside the fibres and hot water in a shell. The scheme of the test rig is shown in Figure 2. The red line represents hot water and the blue line cold water. Hot water was stored in a water tank and then pumped into the shell of the PHFHE through the control valve, which was controlled by the inlet temperature of the shell according to the temperature limit of the PHFHE, which was 80 °C. Pressure and temperature were measured at the inlet and outlet. The flow meter was placed behind the PHFHE. After that, the water was heated by the heater and stored in the water tank. Cold water was taken from the water main. The valve and pressure reduction valve were placed at the beginning of the cold line so as not to exceed the pressure limit of the PHFHE, which was 4 bar. Then, a flow meter was installed. The pressure and temperature were measured at the inlet and outlet of the hollow fibres. Accuracy of thermocouples was  $\pm 0.4\%$  of the measured values, pressure and differential pressure transducer  $\pm 0.014$  bar and flow meter  $\pm 0.5\%$  of reading. A sight glass was placed in the hot and cold line to monitor the undesirable presence of gas. A photo of the test rig is shown in Figure 3.

As mentioned above, the hot water flowed into the shell and cold water into the fibres. The temperature of hot water was chosen as 80 °C, which is the maximum operating temperature of the heat exchanger. The temperature of the cold water was chosen with regard to technical possibilities of testing facilities where 20 °C is the minimal temperature with a stable water supply. The flow rate in the shell was constant and the fibre flow rate was variable. Testing conditions are given in Table 2.

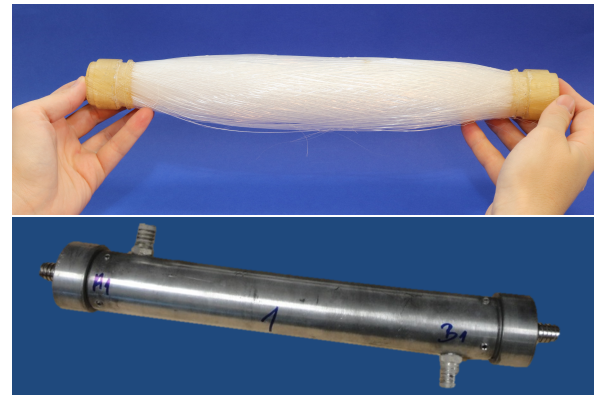


FIGURE 1. Heat transfer insert made of polymeric hollow fibres (top), PHFHE consisting of stainless-steel shell and the polymer hollow fibre insert (bottom).

Sample		AB1	AB2
No. of fibres	[-]	740	820
Fibre outer diameter	[mm]	0.8	0.8
Fibre inside diameter	[mm]	0.64	0.64
Heat transfer area	[m <sup>2</sup> ]	0.52	0.54
Type	[-]	staggered	in-line
Effective length	[mm]	280	260
Temperature limit	[°C]	80	80
Pressure limit	[bar]	4	4
Fibres material	[-]	PC	PC

TABLE 1. Properties of tested samples.

## 3. RESULTS AND DISCUSSION

As mentioned above, temperatures, pressures and flow rates were measured during experiments. The measured data for the heat exchanger AB1 and AB2 are in Table 3. and Table 4. The tables also give the thermal power based on the data measured inside the fibres (for cold water). The error that is listed in the last column then gives the measurement error that is defined as

$$Error [\%] = \frac{Thermal\ power_{shell}}{Thermal\ power_{fibre}} - 1 \quad (1)$$

It can be observed that the error is always below 5%. The accuracy of thermocouples, as already stated, gives the maximal measurement error  $\pm 0.32$  °C for 80 °C measured and the lowest is  $\pm 0.08$  °C for 20 °C measured. The error of the used flowmeter for maximal and minimal flowrate is  $\pm 7.5$  l/h and  $\pm 0.5$  l/h, respectively.

Figure 4 displays the thermal power and the differential pressure on the fibre flow rate. It can be observed that the HE AB1 reaches a higher thermal power at a lower differential pressure with an increasing fibre flow rate than the HE AB2. The thermal power of the AB1 is 5% higher at the maximum fibre flow rate than that of the AB2. The differential pressure is 9% lower for the AB1 than for the AB2. Hence, the structure of the heat transfer insert has

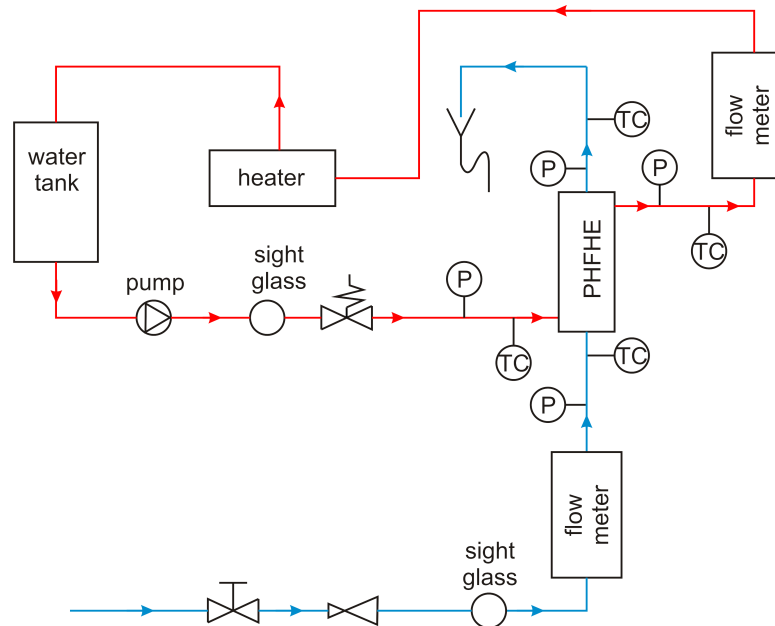


FIGURE 2. Scheme of the test rig (red represents hot water and blue represents cold water, P is for pressure sensor, and TC for temperature probe).

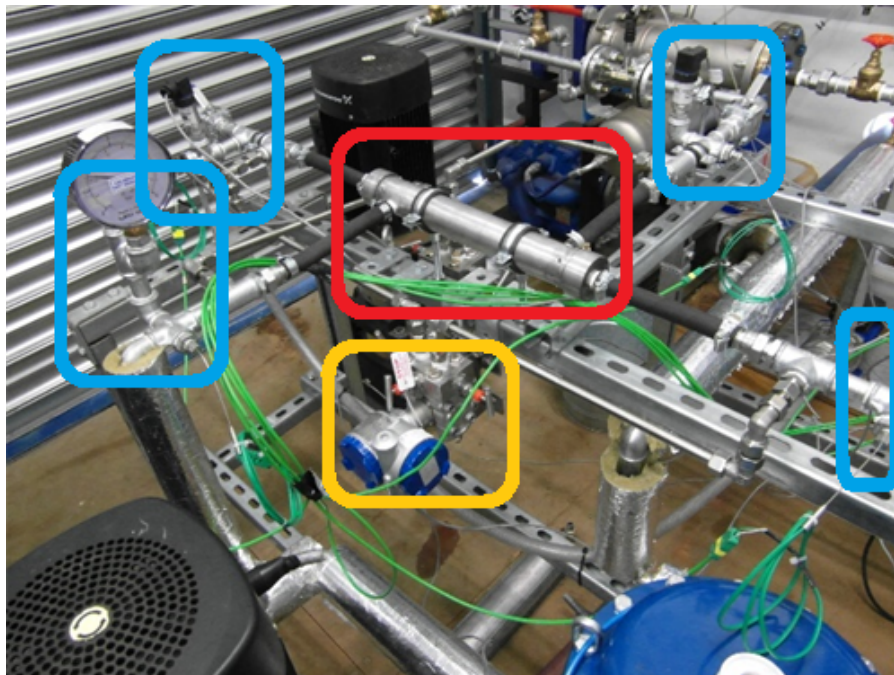


FIGURE 3. Photo of the test rig, tested heat exchanger is in the centre in the red square, the blue square shows the position of thermocouples and pressure meters, the yellow square shows the differential pressure transducer.

Sample	AB1	AB2
Shell temperature [°C]		80
Fibre temperature [°C]		20
Shell flow rate [l·h <sup>-1</sup> ]		1000
Fibre flow rate [l·h <sup>-1</sup> ]	100; 200; 500; 750; 1000; 1500	

TABLE 2. Test parameters.

Shell temperature in	[°C]	80	80	80	80	80	80
Shell temperature out	[°C]	75	70	64	62	61	60
Shell flow rate	[l/h]	1000	1000	1000	1000	1000	1000
Shell diff. pressure	[kPa]	21	21	21	21	21	21
Fibre temperature in	[°C]	20	20	20	20	20	20
Fibre temperature out	[°C]	76	71	51	44	39	34
Fibre flow rate	[l/h]	100	200	500	750	1000	1500
Fibre diff. pressure	[kPa]	4	9	34	61	100	179
Thermal power	[kW]	6.5	11.9	18.1	21	22.2	23.9
Error		-2%	-2%	3%	0%	0%	-2%

TABLE 3. Measured data for AB1 – staggered fibres.

Shell temperature in	[°C]	80	80	80	80	80	80
Shell temperature out	[°C]	74	70	65	63	62	61
Shell flow rate	[l/h]	1000	1000	1000	1000	1000	1000
Shell diff. pressure	[kPa]	21	20	20	20	20	21
Fibre temperature in	[°C]	20	20	20	20	20	20
Fibre temperature out	[°C]	77	69	50	42	38	33
Fibre flow rate	[l/h]	100	200	500	750	1000	1500
Fibre diff. pressure	[kPa]	4	10	35	63	100	197
Thermal power	[kW]	6.7	11.4	17.5	19.3	21	22.8
Error		5%	2%	0%	3%	0%	-3%

TABLE 4. Measured data for AB2 – in-line fibres.

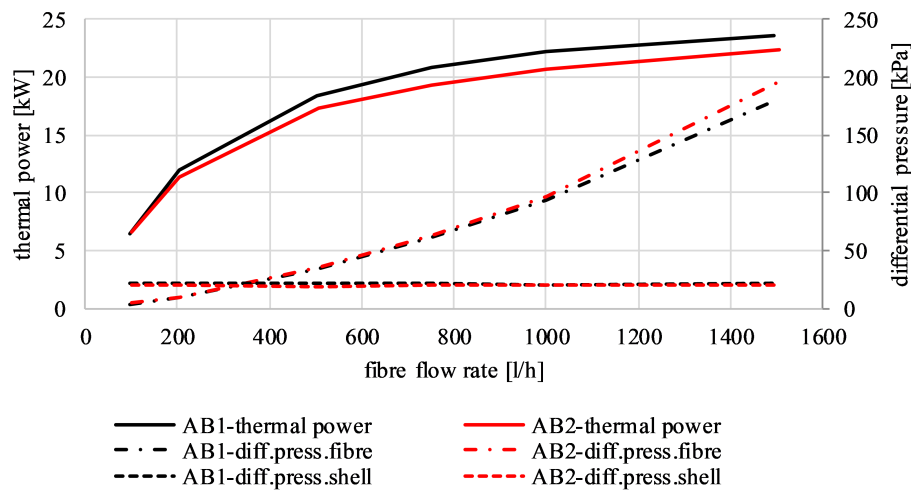


FIGURE 4. Dependence of the thermal power and differential pressure on the fibre flow rate.

Sample		AB1	AB2	difference between AB1 and AB2 in %
Overall HTC at the limit 50 kPa	$[\text{W}(\text{m}^2\text{K})^{-1}]$	1032	914	13 %
Overall HTC at the limit 100 kPa	$[\text{W}(\text{m}^2\text{K})^{-1}]$	1043	934	12 %
Thermal power at the limit 50 kPa	[kW]	20.8	19.3	8 %
Thermal power at the limit 100 kPa	[kW]	22.2	21	8 %

TABLE 5. Comparison of the results at the same differential pressure level.

a beneficial influence, when the fibres are staggered. This reduces the operating costs.

The differential pressure is one of the key parameters of a heat exchanger. Two differential pressure levels were chosen for comparing the samples, 50 kPa and 100 kPa. The heat transfer coefficient (HTC) and thermal power were compared. It can be observed in Fig. 4 that the differential pressure in the shell is always lower than these levels (it reaches the value of 20 kPa). Therefore, the differential pressure inside the fibres is taken into account. Table 5 gives this comparison.

The thermal power is calculated as

$$\text{Thermal power} = \text{flow rate} \cdot c_p \cdot (T_o - T_i) \quad (2)$$

where  $c_p$  is specific heat capacity and  $T$  is temperature, the subscripts  $o$  and  $i$  mark outlet and inlet, respectively. The overall HTC is calculated as

$$\text{Overall HTC} = \frac{\text{Thermal power}}{A \cdot \text{LMTD}} \quad (3)$$

where  $\text{LMTD}$  is logarithmic mean temperature difference and  $A$  is the heat transfer

$$A = N \cdot \pi \cdot D_0 \cdot L \quad (4)$$

where  $N$  is number of fibres,  $D_0$  is outer diameter of fibres, and  $L$  is fibre length.

It can be observed that the differential pressure inside the fibres is up to 50 kPa for a fibre flow rate below 600 l/h. The thermal power at this limit is approximately 20 kW. Therefore, these heat exchangers can be used for small flow rate applications.

#### 4. CONCLUSION

Two heat exchangers were compared. They differ in the structure of the heat transfer insert. One sample has in-line fibres and the second sample has staggered fibres that form an angle of 45° across the layers. Two levels of differential pressure were chosen for their comparison, 50 kPa and 100 kPa. The study shows that the structure of the heat transfer insert significantly influences heat transfer. The thermal power was increased by 13 % when the staggered structure was used in comparison to the in-line fibres. The heat transfer coefficient increased by 8 %.

The study also shows that the thermal power increases too slowly to be useful after the differential pressure drop reaches 50 kPa. However, the differential pressure increases rapidly. The thermal power increased only by 1 % when the differential pressure doubled for the staggered fibres. In the case of in-line fibres, the thermal power increased by 2 %. Hence, the heat exchangers are optimally operated up to the 50 kPa differential pressure level.

#### ACKNOWLEDGEMENTS

This work was supported by the Ministry of Education, Youth and Sports of the Czech Republic under OP RDE grant number CZ.02.1.01/0.0/0.0/16\_019/0000753 “Research centre for low-carbon energy technologies”.

#### REFERENCES

- [1] D. Zarkadas, K. Sirkar. Polymeric hollow fiber heat exchangers: An alternative for lower temperature applications. *Industrial & Engineering Chemistry Research* **43**(25):8093–8106, 2004. DOI:10.1021/ie040143k.
- [2] I. Astrouski, M. Raudensky. The study of polymeric hollow fiber heat exchangers. In *Engineering mechanics 2012*, pp. 47 – 57. 2012.
- [3] T. Brozova, M. Raudensky. Determination of surface wettability of polymeric hollow fibres. *Journal of Elastomers & Plastics* **50**(8):737 – 746, 2018. DOI:10.1177/0095244318765041.
- [4] M. Raudenský, I. Astrouski, M. Dohnal. Intensification of heat transfer of polymeric hollow fiber heat exchangers by chaotisation. *Applied Thermal Engineering* **113**:632 – 638, 2017. DOI:10.1016/j.applthermaleng.2016.11.038.
- [5] I. Astrouski. *Polymeric hollow fiber heat exchanger design*. Ph.D. thesis, Brno University of Technology, 2016.
- [6] T. Brozova, E. Bartuli. Influence of condensation on the outer surface of polymer hollow fiber heat exchangers during heat transfer. vol. ASME 2018 of *16th International Conference on Nanochannels, Microchannels, and Minichannels*. 2018. DOI:10.1115/ICNMM2018-7728.
- [7] I. Krásný, I. Astrouski, M. Raudenský. Polymeric hollow fiber heat exchanger as an automotive radiator. *Applied Thermal Engineering* **108**:798 – 803, 2016. DOI:10.1016/j.applthermaleng.2016.07.181.
- [8] K. Weiß, I. Astrouski, M. Reppich, M. Raudenský. Polymeric hollow-fiber bundles as immersed heat exchangers. *Chemical Engineering & Technology* **41**(7):1457 – 1465, 2018. DOI:10.1002/ceat.201700014.
- [9] I. Astrouski, M. Raudensky, M. Dohnal. Fouling of polymeric hollow fiber heat exchanger by wastewater. *Chemical Engineering Transactions* **45**:949–954, 2015. DOI:10.3303/CET1545159.
- [10] T. Brožová, T. Luks, I. Astrouski, M. Raudenský. Fatigue testing of polymeric hollow fibre heat transfer surfaces by pulsating pressure loads. In *Engineering Mechanics 2015*, vol. 821 of *Applied Mechanics and Materials*, pp. 3–9. Trans Tech Publications Ltd, 2016. DOI:10.4028/www.scientific.net/AMM.821.3.
- [11] P. Bulejko. Numerical comparison of prediction models for aerosol filtration efficiency applied on a hollow-fiber membrane pore structure. *Nanomaterials* **8**:447, 2018. DOI:10.3390/nano8060447.
- [12] T. Sverak, P. Bulejko, J. Ostrezi, et al. Separation of gaseous air pollutants using membrane contactors. *IOP Conference Series: Earth and Environmental Science* **92**:012061, 2017. DOI:10.1088/1755-1315/92/1/012061.
- [13] P. Bulejko, T. Svěrák, M. Dohnal, J. Pospíšil. Aerosol filtration using hollow-fiber membranes: Effect of permeate velocity and dust amount on separation of submicron TiO<sub>2</sub> particles. *Powder Technology* **340**:344 – 353, 2018. DOI:10.1016/j.powtec.2018.09.040.